SUPPLEMENTAL MATERIAL

Expanded Methods and materials

Cortical neurons isolation and culture in microfluidic devices

Cortical neurons were harvested from embryonic day-18 Wistar rats (Charles River Laboratories, Wilmington, MA). Briefly, embryos were removed, and from each, the cerebral cortices were dissected, stripped of meninges, and dissociated with a combination of Ca^{2+}- and Mg^{2+}- free Hanks balanced salt solution (HBSS) containing 0.125% trypsin digestion for 15 minutes, and then mechanically triturated for ~20 times. The triturated cells were passed through a 40 μm cell strainer and counted to obtain a concentration of 3×10^7cells/ml according to published protocols[14, 15].

Two types of axonal microfluidic chamber devices were used in this study: 1) Standard Device (Standard Neuron Device, Cat# SND450, Xona Microfluidics, Temecula, CA) [16, 17] was used to separate axons from neuronal soma. Briefly, cleaned, sterilized, and dried chambers were affixed to poly-D-lysine (PDL) (Sigma-Aldrich, CA) -coated dishes (35mm, Corning). The cortical neurons were plated at a density of 6×10^5cells/chamber in DMEM with 5% FBS for 24 hours. After that, cell culture was incubated with the addition of neurobasal growth medium, 2% B-27, 2mM GlutaMax, and 1% antibiotic-antimycotic (Thermo Fisher Scientific, Waltham MA), which was counted as a starting day in vitro (DIV). On DIV 3, one-half of the medium was replaced with culture medium containing 20 μM 5-fluorodeoxyuridine. The growth media was changed every other day thereafter. 2) Triple Chamber Device (Triple Chamber Neuron Device, Cat# TCND500, Xona Microfluidics, Temecula, CA) [17] was used to separate axons from somata into the distal axon and proximal axon compartments by distal microgrooves and proximal microgrooves, respectively. The seeding of cortical neurons in triple-compartmental microfluidic device used the same protocol as the aforementioned Standard Device, whereas axons required additional time to reach the distal axon compartment.

Animal model

Young adult male Wistar rats were subjected to transient (1 hour) middle cerebral artery occlusion (tMCAO). Briefly, under the operating microscope (Carl Zeiss, Inc., Thornwood, NY, USA), the right common carotid arteries (CCA), the right external carotid artery (ECA) and the internal carotid artery (ICA) of rat were isolated. An 18-19 mm length (determined

by body weight) of 4-0 surgical nylon suture with an expanded (heated) tip was gently advanced from the ECA into the lumen of the ICA to block the origin of middle cerebral artery (MCA). The filament was withdrawn 1h after MCAO.

Primary culture of rat CECs

Briefly, the cerebella, white matter, meninges were removed under a microscope. The cerebral cortex and subcortex of non-ischemic rats (sham operated rats) and the peri-infarct region of cortex and subcortex of stroke rats were cut into small pieces in a RPMI1640, and rinsed twice to remove the blood. The tissues were homogenized with a loose fitting homogenizer for 2-3 strokes. The homogenates were resuspended in 15% dextran (Sigma-Aldrich, 00893) and centrifuged at 10,000 *g* for 15 minutes to collect the pellet. The 0.1% collagenase/dispase with 2% FBS was used to digest the pellet for 6~8 hours and then sent for centrifugation in a colloidal silica gradient solution of 45% Percoll at 20,000 *g* for 20 minutes. The uppermost band with single cells and fragments of microvessels were carefully collected. The CEC culture was initialed on Collagen I (BD Biosciences, Bedford, MA, USA) coated plates. Cultures were maintained in CEC growth medium [20, 21]. The CEC growth medium was made based on MCDB131 medium (Thermo Fisher Scientific) and supplemented with 30μg/ml endothelial cell growth supplement (ECGS, Sigma), 10% FBS, 15U/ml Heparin (Thermo Fisher Scientific), 325μg/ml glutathione (Thermo Fisher Scientific), 1μl/ml 2-mecaptoethanol (Sigma), 1% Antibiotic-Antimycotic (Thermo Fisher Scientific). The primary CECs were cultured in endothelial growth medium for 4 to 7 days when CECs reached approximately 60% confluence. Then, fetal bovine serum (FBS) was replaced with exosome depleted FBS (System Biosciences, CA) for additional 48~72 hours. After that, the medium was collected for isolation of exosomes. Passage 1 to 2 endothelial cells were employed in the current study to generate exosomes.

Isolation and characterization of exosomes from CECs

Briefly, the growth medium supernatant was passed through a 0.22μm filter (Millipore, CA) to filter out dead cells and large debris. A 10,000*g* centrifugation for 30 minutes was performed to further remove small debris. After a 100,000*g* centrifugation for 3 hours, exosomes were collected. The pellet was diluted by sterilized PBS. The particle numbers and size of harvested CEC-exos were analyzed using a Nanosight (NS300, Malvern

Panalytical, UK). Briefly, gradient dilutions (1:10, 1:100 and 1:1000) of exosomes in distilled water were used for nanoparticle tracking analysis (NTA) by means of Nanosight system with NTA 3.3 Dev Build 3.3.104 software. The camera level was set to 12 to 15 in order to balance signal contrasts and backgrounds. Three 30-second long videos were recorded via a SOP-type procedure with default options for standard measurements. Over 500 particles counted in each video were considered as validated for data analysis.

To further characterize exosomes, we examined the ultra-structural morphology of exosomes by means of transmission electron microscope (TEM, Phillips, EM208). Briefly, fresh collected exosomes in PBS were applied on the formvar carbon films covered copper grids (400mesh, FCF400-Cu, EMS, Hatfield, PA) for 45 seconds to allow attachment. After two rinses with distilled water to remove the unattached particles, the grids were counter stained in 1% Osmium tetroxide (OsO4) for 30 seconds. The grids were then imaged under TEM.

Western blot analysis was performed to characterize proteins in collected exosomes. Total proteins from exosomes were collected using 2X lysis buffer (RIPA, SigmaAldrich, MO) to lyse exosomes samples. The following primary antibodies were used: mouse monoclonal anti-Alix (1:500; 2171, Cell Signaling), rabbit polyclonal anti-CD63 (1:500; sc-15363, Santa Cruz), rabbit polyclonal anti-CD31 (1:500, MAB1393, Anti-PECAM-1, EMD Millipore), rabbit polyclonal anti-ZO-1 (1:500; 61-7300, Thermo Fisher Scientific), and rabbit monoclonal anti-Calnexin (1:500, 699401, Biolegend).

Analysis of axonal growth

Total axonal length in axonal compartment. Briefly, the distal axons in the axonal compartment were imaged under a 10x objective of a light microscope (IX71, OLYMPUS, Tokyo, Japan) equipped with a CCD camera (CoolSnap, 5000) and MetaView software (Universal Imaging, West Chester, PA). Five images per compartment were acquired, which encompass the majority of the compartment. The lengths of the 15 longest axons in each compartment were measured by tracing individual axons using imageJ according to the published procedures[15, 23, 24]. We previously demonstrated that this method reliably provides overall axonal lengths within the axonal compartment[15, 22, 23].

Growth cone extension. A time-lapse microscope, which was equipped with a 5% CO_2 at

37°C top chamber (Live-Cell Control Unit) on the motorized z-stage of the TE2000-U inverted microscope (Nikon), was employed to analyze growth cone extension. Approximately, 40 growth cones were imaged during the 60 minutes period from 6 individual chambers of each experimental group. Each image was acquired at a 5 minute interval, and distance changes of growth cones within acquired images during 60 minutes were calculated by means of Metamorph software (Universal Imaging, West Chester, PA).

Analysis of axonal transport

Lsotracker at 10μM was applied into the distal axon compartment of TCND500 for 2 hours before image acquisition. The movement of fluorescent particle signals localized to the distal microgrooves was recorded using the time-lapse microscope consecutively for 50 images at 800 ms per image under a 40x objective with 1.5x magnification. Images were processed into kymographs, and the bidirectional movement velocity of every fluorescent signal was analyzed using ImageJ[25].

Exosome labeling

Exosome labeling by Exo-fect exosome transfection kit (System Bioscience, CA) [22]. Briefly, 3×10^{10} exosomes (about 100μg proteins) were incubated with transfection solution and siRNA at 37^0C for 10 minutes in a shaker. Transfected exosomes were then collected by centrifugation at 13,000 rpm and re-suspended with 100 μl PBS and were applied to the axonal compartment within 10 minutes. Fluorescent signals within axons were detected by means of a laser-scanning confocal microscope (Zeiss LSM 510 NLO, Carl Zeiss, Germany) Exosome labeling by GFP. Briefly, nCECs were transfected with a plasmid carrying pEGFP-CD63 vector (CD63-pEGFP C2) by means of electroporation[15] (Nucleofector system, program U11, Lonza). The exosomes were isolated from the collected supernatant by differential ultracentrifugation. CD63 is a membrane protein marker of exosomes [26]. The presence of GFP proteins in exosomes (CEC-GFP-exos) was examined by means of Western blot. CD63-pEGFP C2 was a gift from Paul Luzio (Addgene plasmid # 62964; http://n2t.net/addgene:62964 ; RRID:Addgene_62964).

Exosome Immunogold staining

Briefly, axons and their cell bodies were grown on the Aclar plastic film (EMS, Hatfield, PA) in the axonal and soma compartments of microfluidic devices , respectively,.

CEC-GFP-exos were placed into the axonal compartment for 4 hours. After that, the axons and neurons were fixed with 2.5% glutaraldehyde 1.25% paraformaldehyde and 0.03% picric acid in 0.1 M sodium cacodylate buffer (pH 7.4). Postfixation was performed for 30 minutes in 1% Osmium tetroxide (OsO4)/1.5% Potassium ferrocyanide (KFeCN6). After dehydration in grades of alcohol, the samples were embedded in TAAB Epon (EMbed 812 Kit, EMS) and polymerized at 60^0 C for 48 hours. After removing the Aclar, ultrathin sections (80 nm) were cut and loaded on nickel grids (400 square mesh, EMS). Immunogold staining was performed on the grids with 2% anti-rabbit monoclonal antibody against GFP (G10362, ThermoFisher) and 10 nm gold conjugated streptavidin (25269, EMS). The grids were imaged under the TEM (Phillips, EM208).

Knockdown of Dicer

nCECs were transfected with a shRNA against Dicer plasmid (sc-40489-SH, Santa Cruz) by means of electroporation. nCECs transfected with control shRNA (sc-108060, Santa Cruz) plasmid were used as a control. The supernatant was collected from transfected nCECs cultured with Exo-free FBS for 48 hours. The exosomes were then isolated by means of differential ultracentrifugation (dp-Dicer-exos).

Fluorescent In situ hybridization (FISH)

Cultured neurons in SND450 were fixed with 4% paraformaldehyde. A further fixation with 1-ethyl-3-(3-dimethylaminopropyl) carbodiimide (EDC) was applied to reduce the loss of miRNAs during processing[27]. Digoxigenin-labeled LNA probes at 0.25 μM in hybridization buffer were used. Signals were detected by incubation of the cells in solution containing Fluorophore Amplification Reagent Working Solution (TSA PLUS Fluorescence Kits, PekinElmer).

Immunocytochemistry

After washing with PBS twice and fixation with 4% formaldehyde, axons and neurons in the microfluidic devices were incubated with the primary antibodies for one or two nights at 4ºC, and then with Cy3 or FITC conjugated secondary antibodies for 2 hours at room temperature. Nuclei were counterstained with 4',6-diamidino-2-phenylindole (DAPI, 1:10,000, Vector Laboratories, Burlingame, CA). The following primary antibodies were used: a monoclonal antibody against phosphorylated neurofilament heavy chain (pNFH,

SMI31, 1:500 Covance); a rabbit polyclonal anti-CD31 (1:500, MAB1393, Anti-PECAM-1, EMD Millipore), a rabbit polyclonal anti-zo-1 (1:500, 61-7300, Thermal Fisher Scientific). The immunoreactive cell bodies and axons of the cortical neurons were imaged under a 63x objective by means of a laser-scanning confocal microscope (Zeiss LSM 510 NLO) [19].

Western blot analysis

Due to a small volume of proteins that can be extracted from the axonal compartment of the microfluidic device, each protein sample was collected by pooling from 4 to 6 axonal compartments of individual devices. Briefly, for axonal protein collection, in order to minimize contamination from the cell body compartment, 100 µl of PBS was added into the cell body compartment, which prevents any buffer in the axonal compartment to flow back to the cell body compartment. Then, 10 µl of lysis buffer (RIPA, SigmaAldrich, MO) was applied to the axonal compartment for 10 minutes. During the entire period, the chamber was placed on ice. To obtain sufficient amount of proteins for blotting, axonal samples from 4 to 6 chambers were pooled for one blot. Protein concentrations of the supernatants of the cell body and axonal extracts were determined using a bicinchoninic acid (BCA) protein assay kit (Pierce Biotechnology, Rockford, IL). Western blots were performed according to published methods [14,15]. Briefly, equal amounts of total protein for each sample were loaded on 10% SDS-polyacrylamide gels. After electrophoresis, the protein was transferred to nitrocellulose membranes, and the blots were subsequently probed with the following primary antibodies: rabbit polyclonal anti-Sema6A (1:500; ab154938, Abcam), rabbit polyclonal anti-PTEN (1:1000; 9559, Cell Signaling), rabbit polyclonal anti-PI3 kinase p85 (1:1000; 06-496, Millipore), rabbit polyclonal anti-RhoA (1:1000; 10749-1-AP, ProteinTech) and mouse monoclonal anti β-actin (1:10,000; ab6276, Abcam, Cambridge, MA). For detection, horseradish peroxidase-conjugated secondary antibodies were used (1:2000) followed by enhanced chemiluminescence development (Pierce Biotechnology). Protein levels of β-actin and PI3K subunit p85 were used as the internal controls for somata and axons, respectively [15]. Western blots were performed from at least 3 individual experiments. The optical density of protein signals was quantified using an image processing and analysis program (Scion image, Ederick, MA).

miRNA PCR Array and Real-Time Reverse Transcriptase-Polymerase Chain

Reaction.

RNA in exosomes was extracted from exosomes isolated from three individual batches of nCECs or isCECs. Each batch of nCECs or isCECs was obtained by preparing CECs isolated from 4 normal or ischemic rats. RNA in axons was extracted from axons treated by three individual batches of nCEC-exos or isCEC-exos. Each sample was collected by pooling RNAs from 4 to 6 axonal compartments of individual devices. Totally, there are 3 different batches of either nCEC-exos or isCEC-exos and three different exosome-treated axons. For each sample, the results of the PCR array, are presented by an individual column of heatmap in Fig.2 and Supplemental Fig. IV. Briefly, the total RNAs at 1.5 to 2.0 μg were harvested from the axonal or cell body compartment of 20 microfluidic culture devices per experimental group, or from $3x10^{11}$ particles of CEC-exos, respectively. Reverse transcription (RT) was then performed using miScript HiSpec Buffer (miScript II RT Kit, Qiagen). cDNA prepared in a RT action and served as the template for the real-time PCR analysis using the miRNA PCR array kit (MIRN-107ZE-1, Qiagen) and the miScript SYBR Green kit on an ABI ViiATM 7 PCR instrument (Applied Biosystems). A standard cycling condition was used, which includes PCR initial activation for 15 minutes, and following 3-step cycling (denaturation for 15 seconds; annealing for 30 seconds and extension for 30 seconds). The cycle number was set to 45 according to the amount of template cDNA, so that Ct value greater than 40 is considered to be below the detection level according to the array manual. Six small nucleolar RNAs (SNORD61, 68, 72, 95, 96 and RNU6B/RNU6-2) were used as normalization controls. Data analysis was performed using online data analysis software (https://www.qiagen.com/us/shop/genes-and-pathways/data-analysis-center-overview-page/). The fold changes of each miRNA from experimental samples to the control samples were calculated using $2^{(-\Delta\Delta Ct)}$ method[33]. The ΔCt was calculated using the formula $\Delta Ct=Ct^{miRNA}$-Average Ct^{snRNAs} . The ΔΔCt was calculated using $\Delta\Delta Ct=\Delta Ct^{sample}-\Delta Ct^{control}$.

TaqMan miRNA assays were used with the following specific primers of: miR-19a (mature sequence: UGUGCAAAUCUAUGCAAAACUGA), miR-27a (mature sequence: UUCACAGUGGCUAAGUUCCGC), miR-298 (mature sequence:

GGCAGAGGAGGGCUGUUCUUCCC), miR-346 (mature sequence: UGUCUGCCUGAGUGCCUGCCUCU), miR-125b (mature sequence: UCCCUGAGACCCUAACUUGUGA), miR-34a (mature sequence: UGGCAGUGUCUUAGCUGGUUGU), miR-106b (mature sequence: UAAAGUGCUGACAGUGCAGAU), miR-195 (mature sequence: UAGCAGCACAGAAAUAUUGGC). U6, RNU19 and RNU48 were used as normalization controls. Analysis of gene expression was carried out using the $2^{(-\Delta\Delta Ct)}$ method [28]. The ΔCt was calculated using the formula $\Delta Ct=Ct^{miRNA}$-Average $Ct^{U6/RNU19/RNU48}$ miScript Precursor Assays was used with following specific primers: pre-miR-27a (MP00007749), pre-miR-19a (MP00007511), pre-miR-298 (MP00007791), pre-miR-195 (MP00007476). SNORD61 were used as internal control (MS00033705). Briefly, cDNA is prepared using the miScript II RT kit (Qiagen, Valencia, CA) and then amplified with the miScript Precursor Assay kit and miScript SYBR Green kit (Qiagen, Valencia, CA). Analysis of gene expression was carried out using the $2^{(-\Delta\Delta Ct)}$ method [28].

Online Figures

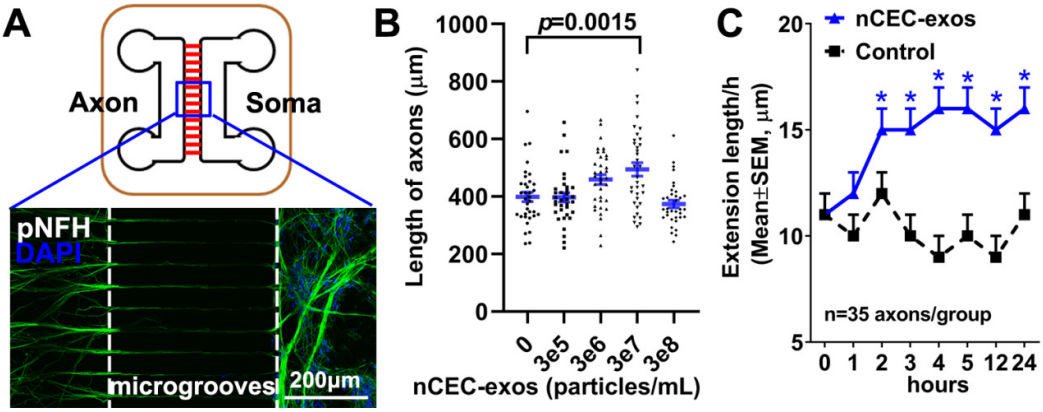

Supplemental Figure I. CEC-exos applied to distal axons promote axonal growth. Schematic figure of the standard microfluidic device along with an immunofluorescent image captured in the box area (**A**) shows cortical neurons grown in the cell body compartment (Soma) and their axons in 450µm long microgrooves and in the axonal compartment (Axon). Quantitative data show the effect of different concentrations of nCEC-exos on average length of axons (**B**) and elongation of axons with time after axonal application of CEC-exos (3e7, $3x10^7$particles/mL, **C**). One-way ANOVA with Tukey's multiple comparisons test was used in B. Student t-test was used in C. * $p<0.05$ vs control. Error bars indicate the standard error of the mean (SEM).

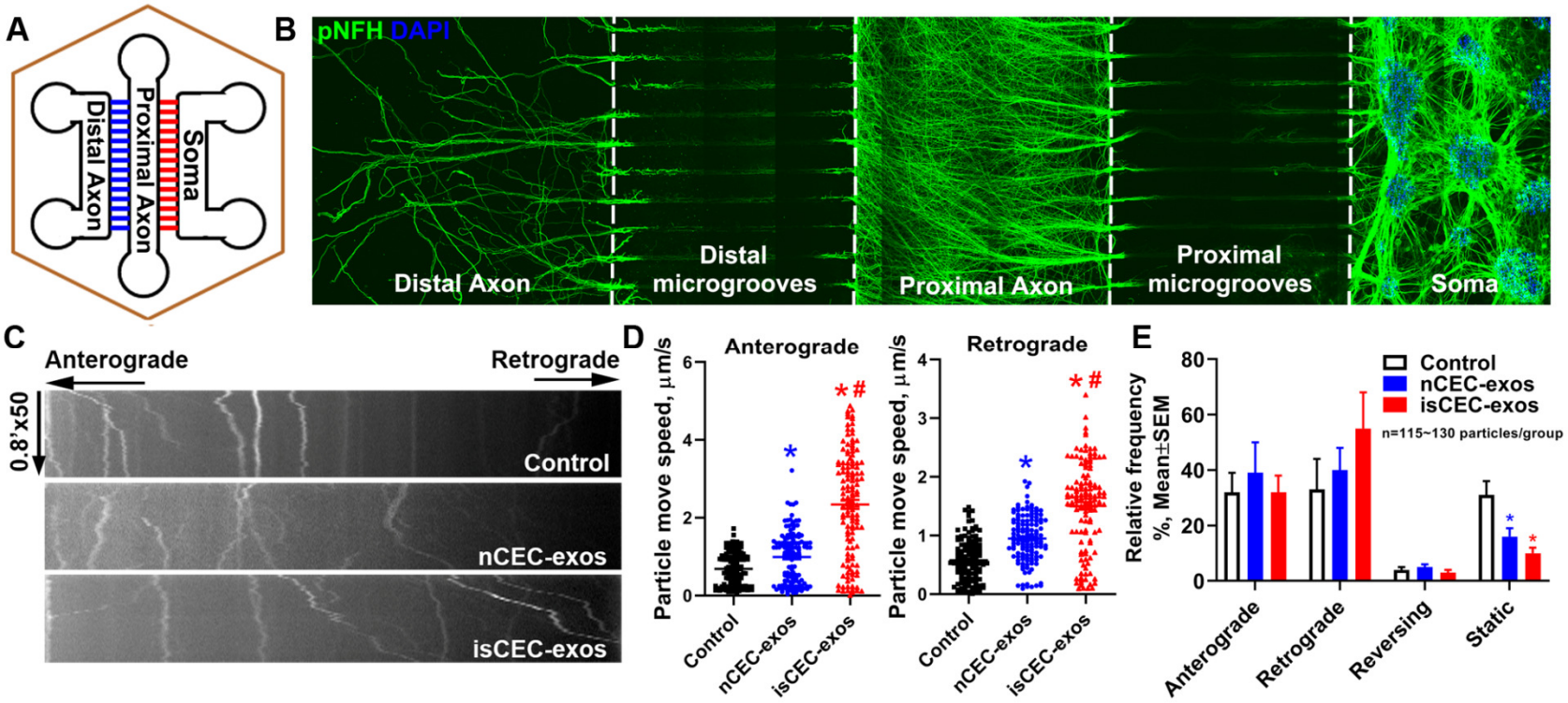

Supplemental Figure II. CEC-exos applied to distal axons promote axonal transport. A schematic shows the triple chamber device including compartments of Soma, Proximal and Distal microgrooves, and Proximal and Distal Axons (**A**). A representative confocal microscopic image of pNFH positive neurons and axons shows that cortical neurons seeded in cell body compartment (Soma) of the triple chamber device extended their axons into the proximal and distal axonal compartments by crossing proximal and distal microgrooves (**B**). Representative Kymograph images (**C**) and quantitative data (**D**) show the effect of nCEC- and isCEC-exos on two-directional movement of lysotracker labeled puncta fluorescent signals (**C**) and on anterograde/retrograde transport velocity (**D**) within axons of distal microgrooves, respectively. Quantitative data show the percentage of the different moving status of puncta fluorescent signals (**E**). Arrows in **C** represent the movement directions of fluorescent signals. One-way ANOVA with Tukey's multiple comparisons test was used. * $p<0.05$ vs control; #, $p<0.05$ vs nCEC-exos. Error bars indicate the SEM.

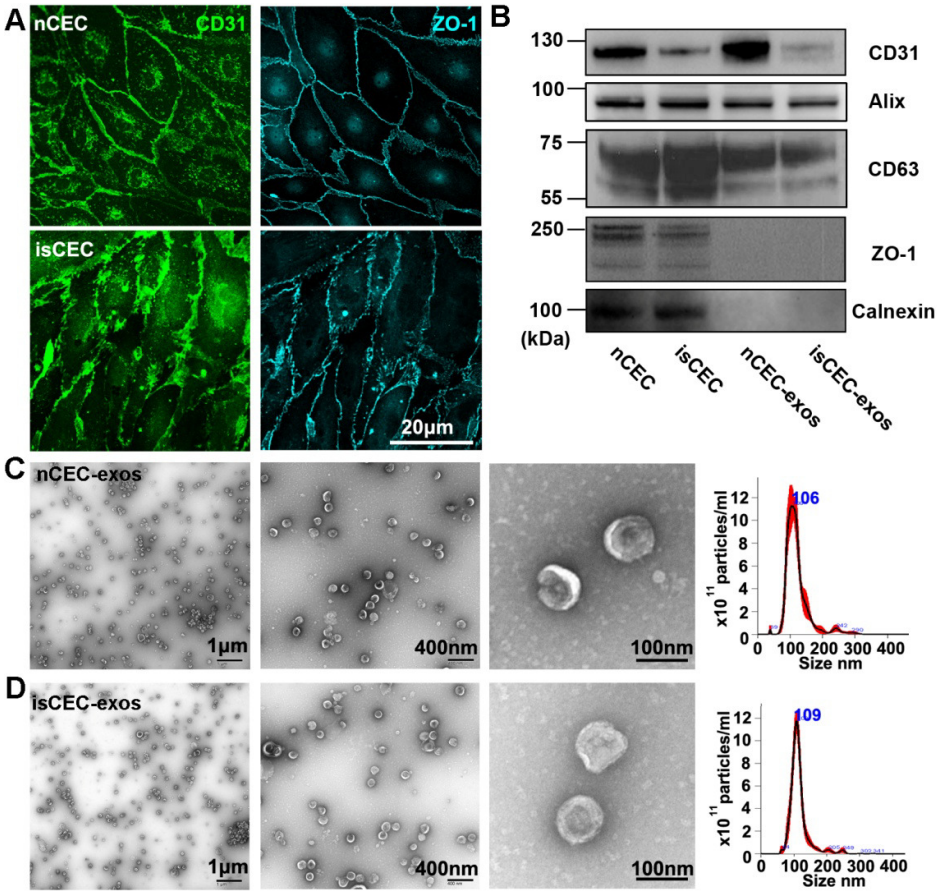

Supplemental Figure III. **Exosomes derived from non-ischemic and ischemic CECs.** Representative confocal microscopic images (**A**) show that primary CECs isolated from non-ischemic adult rats (nCEC) or rats subjected to tMCAO (isCEC), respectively, are positive of endothelial cell and tight junction proteins of CD31 (green, CD31) and ZO-1 (cyan, ZO-1). Western blot (**B**) analysis showed that the vesicles contained CD31 endothelial protein, suggesting that the vesicles are from endothelial cells. The results show these vesicles contained CD63 and Alix proteins, markers of exosomes, but did not show ZO-1 and calnexin proteins, although these two proteins were present in the CECs. Representative TEM images show nCEC-exos (**C**) and isCEC-exos (**D**) have doughnut-shaped vesicles under different magnifications with diameters ~100 nm (C, D), Nanosight data of exosomes show the size distributions of nCEC-exos (**C**) and isCEC-exos (**D**) have a mean diameter of 115±1.3nm and 120±2.2 nm, respectively.

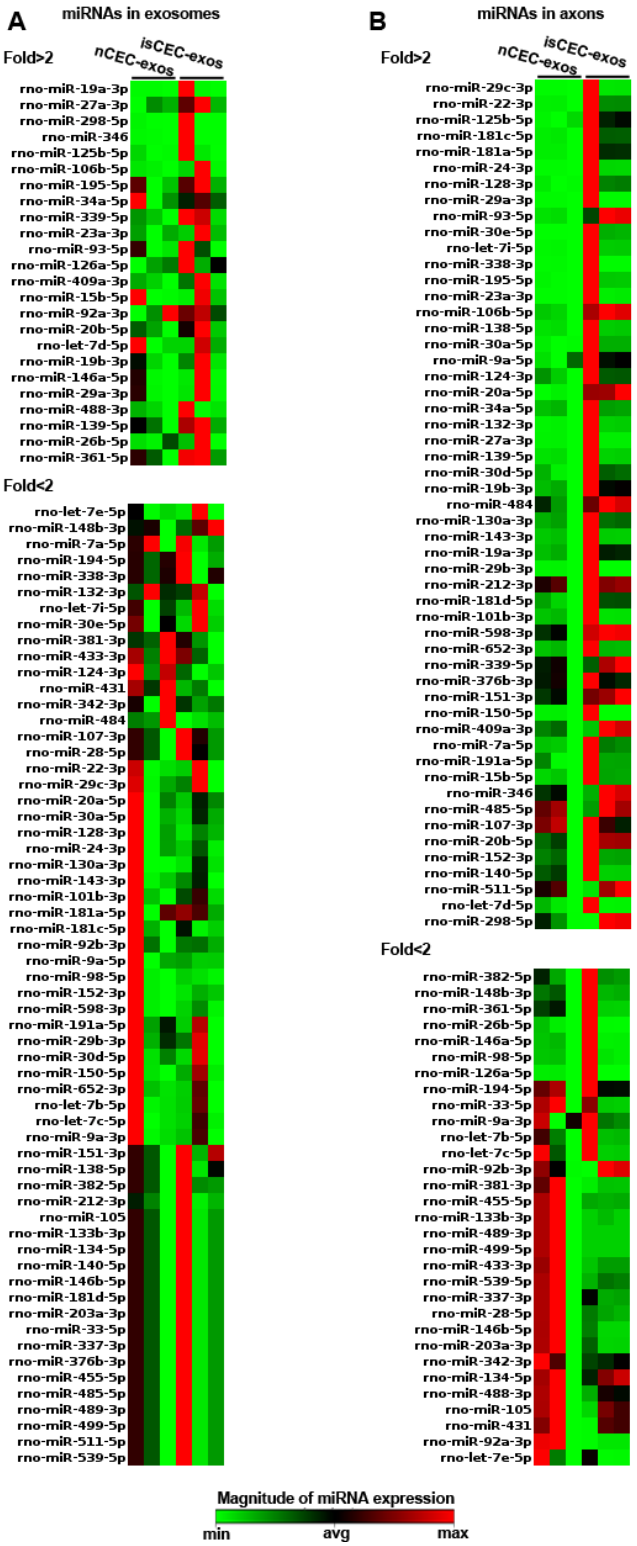

Supplemental Figure IV. The miRNA PCR array data. Heatmaps show miRNAs with > or < 2 fold changes in nCEC-exos and isCEC-exos (**A**) and in axons treated with nCEC-exos or isCEC-exos (**B**). Each column represents individual samples.

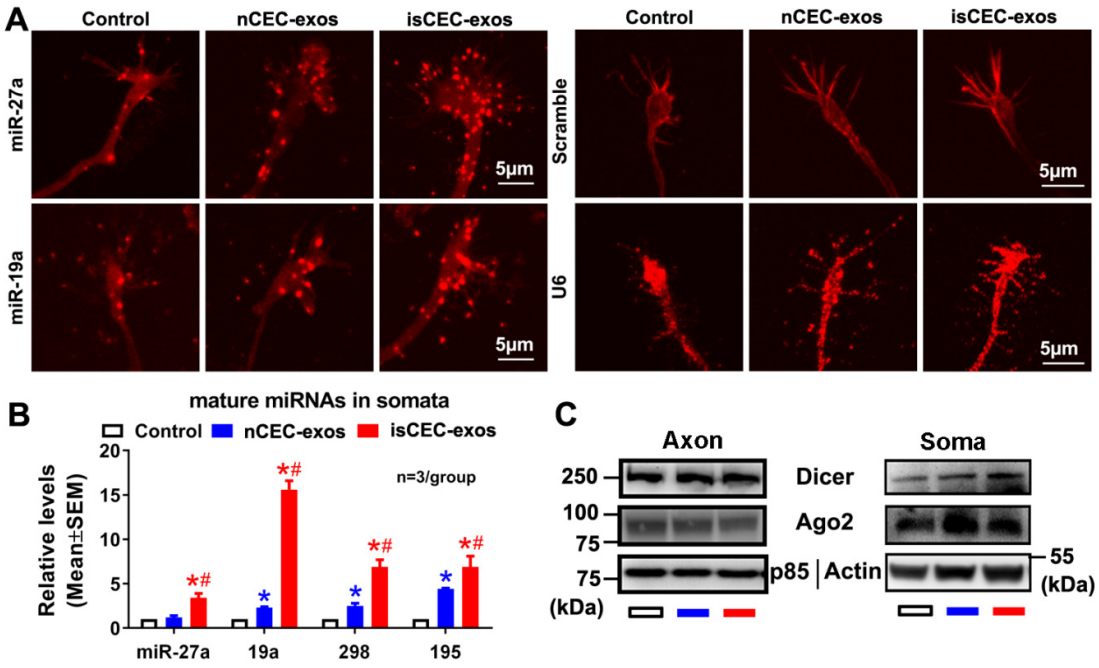

Supplemental Figure V. The effect of CEC-exos on levels of miRNAs and miRNA machinery proteins in distal axons of cortical neurons. Representative FISH images (**A**) show the presence of miR-27a and miR-19a in distal axons after axonal application of nCEC- or isCEC-exos, respectively, whereas miR-27a was not detected by scramble probes (E, scramble), U6 signals were presented (**A**, U6). It appears that U6 signals were strong in axons treated with exos compared with control. Quantitative RT-PCR data show the effect of axonal application of CEC-exos on the levels of mature miRNAs in cell bodies (**B**). Representative Western blot images (**C**) show the effect of axonal application of CEC-exos on the levels of Dicer and Ago2 both in distal axons and somata compared to the control without any treatments. One-way ANOVA with Tukey's multiple comparisons test was used in B. *, $p<0.05$ vs control; #, $p<0.05$ vs nCEC-exos. Error bars indicate the SEM. Data were acquired from 3 independent experiments (N=3/group).

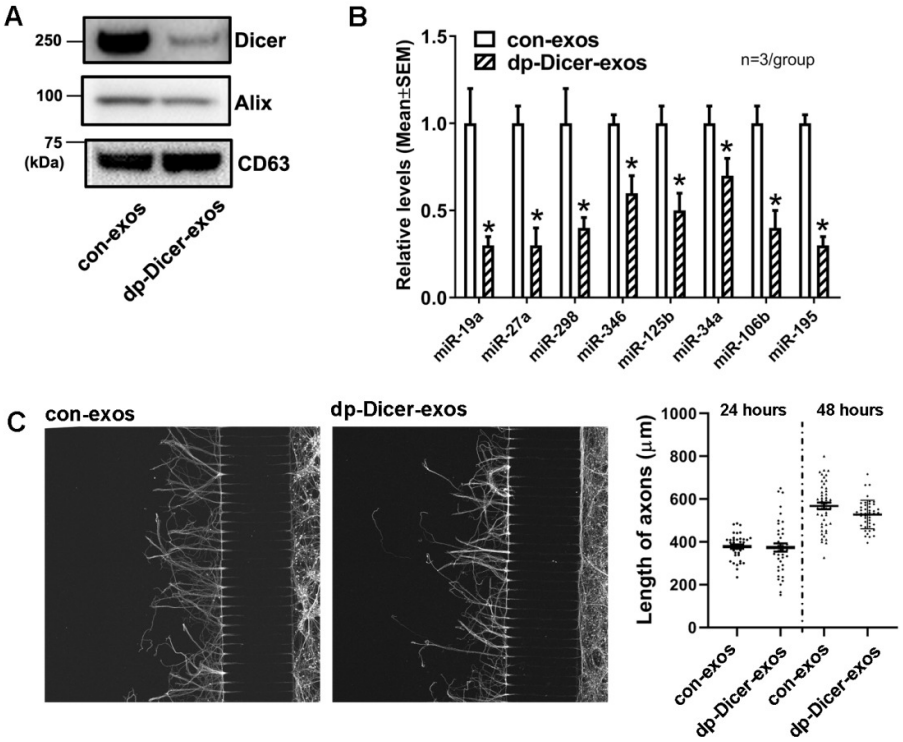

Supplemental Figure VI. The effects of dp-Dicer-exos on axonal growth. Western blot and qRT-PCR results show reduction of Dicer protein (**B**) and miRNAs (**C**), respectively, in dp-Dicer-exos. Representative confocal microscopic images show distal axonal growth at 24 hours after treatments and corresponding quantitative data of distal axonal growth at 24 hours and 48 hours after treatments with con-exos and dp-Dicer-exos, respectively. Error bars indicate the SEM. One-way ANOVA with Tukey's multiple comparisons test was used in **C**. Student t-test was used in **B**. * $p<0.05$ vs control exos. N=3 represents 3 independent experiments.

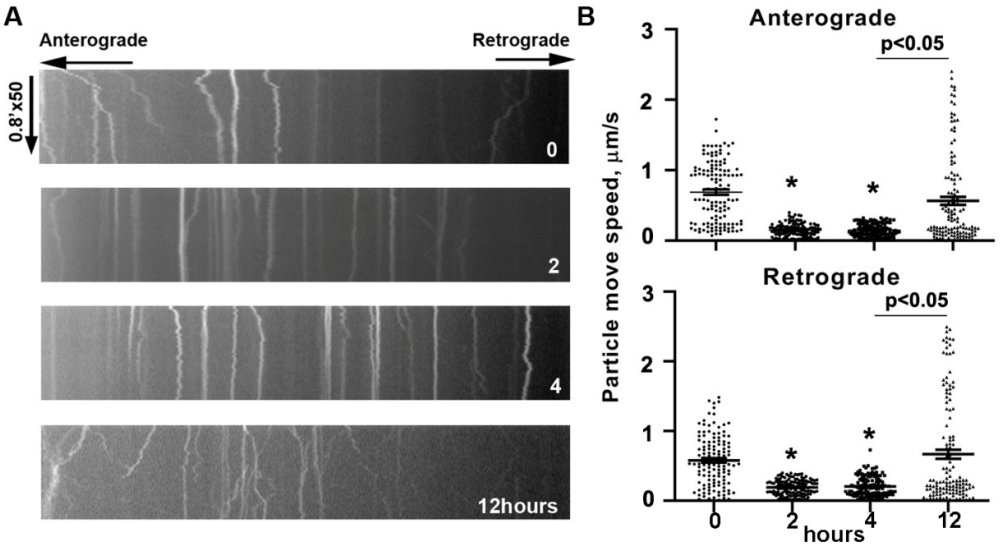

Supplemental Figure VII. The effects of emetine on axonal transport. Representative Kymograph images (**A**) and their quantitative data (**C**) show changes of the two-directional transport velocities at 2, 4, and 12 hours after emetine removal from proximal axon compartment. Error bars indicate the SEM. One-way ANOVA with Tukey's multiple comparisons test was used. *, $p<0.05$ vs control.

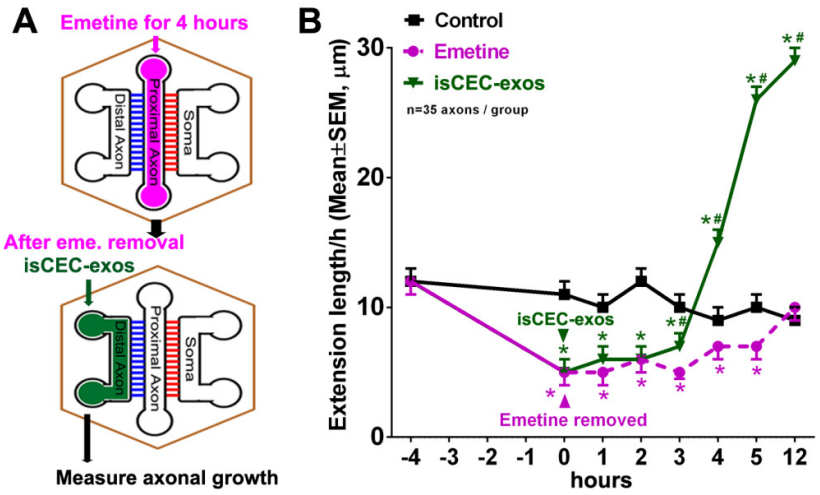

Supplemental Fig VIII. The effect of transient blockage of axonal transport on isCEC-exo-altered axonal growth. A schematic of workflow (**A**) and quantitative data (**B**) shows growth cone extension of distal axons acquired by the time-lapse microscope during a 16 hour period in the control group without any treatments (**B**, control), the transient (4 hours) emetine treated group (**B**, Emetine, from time -4 to 0 hour), and the isCEC-exos group in which isCEC-exos were applied to the distal axon compartment after emetine removal (**B**, isCEC-exos, at time 0 hour).

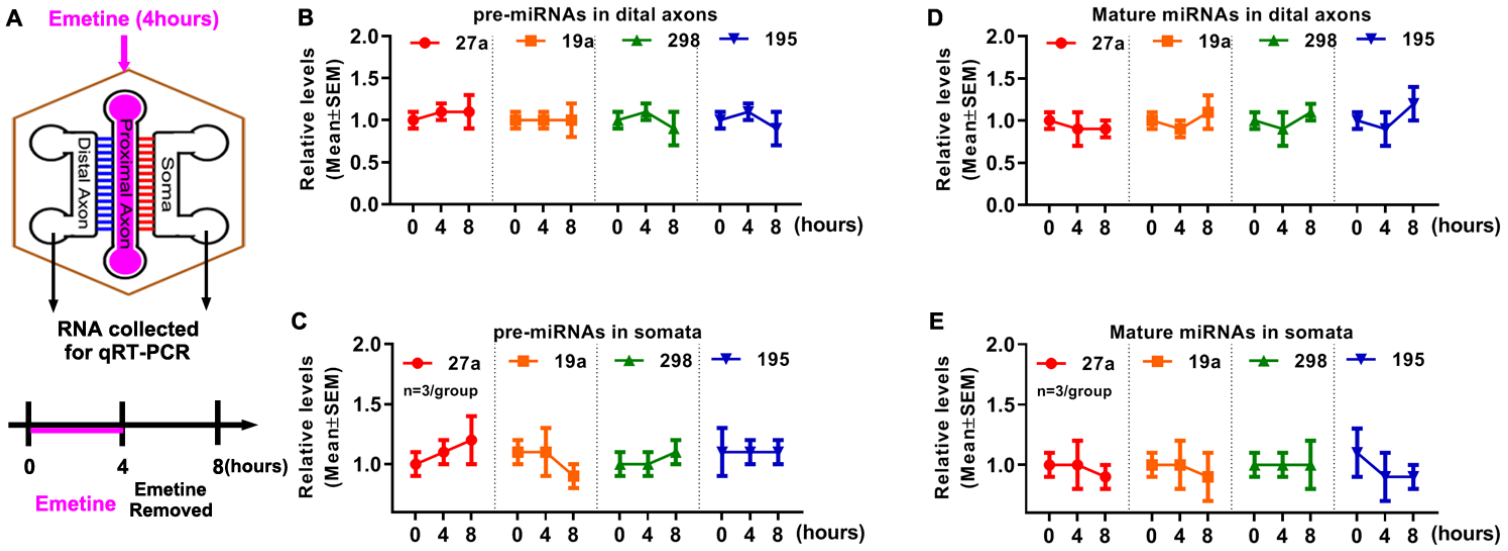

Supplemental Figure IX. The effects of emetine transiently applied to proximal axons on the pre- and mature miRNAs in distal axons and their parental somata. A schematic shows a workflow to collect samples from the distal axonal/somal compartments after transient emetine treatment (**A**). Quantitative RT-PCR results show the precursor (**B,C**) and mature forms (**D,E**) of 4 miRNAs in distal axons and the parental somata at the time points before (0) and 4h after application of emetine in proximal axons (4) and 4h after emetine removal (8 hours).

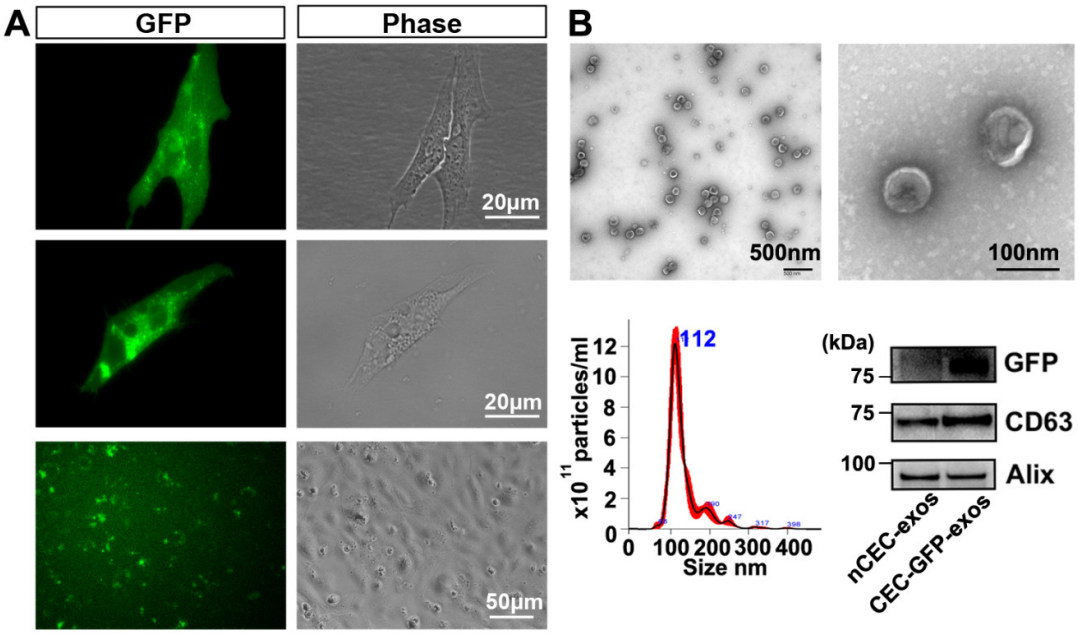

Supplemental Figure X. The CEC-GFP-exos. Fluorescent and bright field phase microscopy images show the CECs expressing GFP-CD63 (**A**). Panel B shows the ultrastructural morphologies, particle size distribution, and cargo proteins of exosomes isolated from the supernatant of transfected CECs (CEC-GFP-exos).

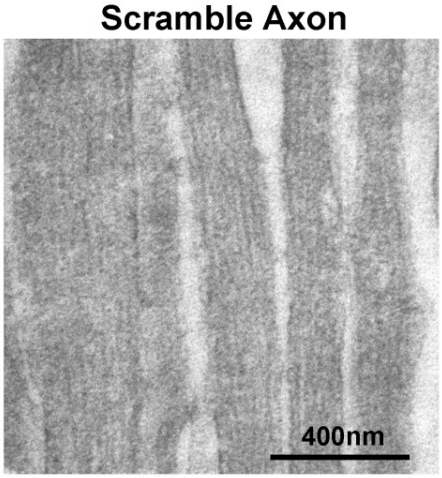

Supplemental Figure XI. GFP positive gold particles in axons were not detected. A representative TEM image shows absence of GFP positive gold particle in the neurofilament of axons (Scramble Axon) when the primary antibody against GFP was omitted.

Online Tables

Supplemental Table I. Abundant miRNAs in nCEC-exos.

miRNAs	Average CT	SD (n=3)	miRNAs	Average CT	SD (n=3)
miR-92a-3p	30.3	1.4	let-7d-5p	38.1	2.0
let-7b-5p	33.4	1.4	miR-652-3p	38.1	1.3
let-7c-5p	34.0	1.9	miR-27a-3p	38.1	1.6
miR-431	34.1	0.6	miR-128-3p	38.3	1.4
miR-381-3p	34.1	0.6	miR-181a-5p	38.4	1.4
miR-433-3p	34.5	0.7	let-7e-5p	38.4	1.5
miR-92b-3p	34.8	0.9	miR-148b-3p	38.4	0.2
miR-342-3p	35.0	1.0	miR-15b-5p	38.4	2.1
miR-124-3p	35.1	0.8	miR-29c-3p	38.5	1.4
miR-126a-5p	35.4	0.9	miR-195-5p	38.6	1.4
miR-125b-5p	35.6	1.5	miR-9a-3p	38.7	1.5
miR-24-3p	35.9	2.6	miR-146a-5p	38.9	2.0
miR-22-3p	36.3	1.9	miR-29a-3p	39.0	1.8
miR-29b-3p	36.3	1.1	miR-598-3p	39.0	1.8
miR-191a-5p	36.4	1.0	miR-98-5p	39.0	1.7
miR-130a-3p	36.5	2.0	miR-132-3p	39.1	0.6
miR-23a-3p	36.5	1.2	miR-9a-5p	39.1	0.9
miR-30a-5p	36.6	1.4	miR-150-5p	39.2	1.3
miR-30d-5p	36.7	1.0	miR-26b-5p	39.4	1.1
miR-34a-5p	37.0	2.3	miR-101b-3p	39.6	0.8
miR-152-3p	37.1	1.8	miR-181c-5p	39.7	0.6
miR-30e-5p	37.2	2.2	miR-19b-3p	39.7	0.6
miR-143-3p	37.3	1.3	miR-298-5p	39.7	0.5
let-7i-5p	37.6	2.1	miR-194-5p	39.8	0.4
miR-20a-5p	37.6	2.0	miR-338-3p	39.8	0.4
miR-93-5p	37.8	2.3	miR-7a-5p	39.8	0.4
miR-484	37.8	1.2			

Supplemental Table II. Abundant miRNAs in isCEC-exos.

miRNAs	Average CT	SD (n=3)	miRNAs	Average CT	SD (n=3)
miR-92a-3p	29.8	0.7	miR-181a-5p	38.3	0.7
let-7b-5p	33.6	1.7	miR-146a-5p	38.4	2.8
let-7c-5p	34.0	1.8	miR-346	38.4	2.8
miR-125b-5p	34.0	3.1	let-7e-5p	38.4	2.7
miR-381-3p	34.5	0.4	miR-29a-3p	38.5	2.6
miR-126a-5p	34.6	0.3	miR-29c-3p	38.5	1.8
miR-431	35.0	0.6	miR-106b-5p	38.7	2.3
miR-92b-3p	35.1	0.5	miR-652-3p	38.7	2.0
miR-433-3p	35.1	0.5	miR-128-3p	38.8	1.1
miR-342-3p	35.4	0.4	miR-9a-3p	38.9	1.7
miR-23a-3p	35.5	1.9	miR-26b-5p	39.0	1.8
miR-34a-5p	35.9	0.8	miR-339-5p	39.0	1.0
miR-22-3p	36.2	2.4	miR-484	39.1	0.8
miR-124-3p	36.3	0.1	miR-150-5p	39.1	1.6
miR-27a-3p	36.3	1.4	miR-19b-3p	39.2	1.4
miR-24-3p	36.3	1.6	miR-409a-3p	39.2	1.3
miR-130a-3p	36.4	1.6	miR-598-3p	39.4	1.1
miR-30a-5p	36.8	1.3	miR-132-3p	39.4	0.9
miR-93-5p	36.8	2.8	miR-20b-5p	39.5	0.9
miR-29b-3p	37.2	2.1	miR-101b-3p	39.5	0.9
miR-30d-5p	37.2	1.7	miR-488-3p	39.5	0.8
miR-30e-5p	37.3	2.1	miR-9a-5p	39.6	0.4
miR-195-5p	37.4	1.2	miR-139-5p	39.6	0.7
miR-152-3p	37.4	1.0	miR-361-5p	39.7	0.6
let-7i-5p	37.5	2.0	miR-151-3p	39.7	0.4
miR-143-3p	37.5	1.2	miR-98-5p	39.8	0.4
let-7d-5p	37.5	1.9	miR-107-3p	39.8	0.4
miR-20a-5p	37.6	1.3	miR-28-5p	39.8	0.3
miR-19a-3p	37.8	2.8	miR-338-3p	39.9	0.3
miR-15b-5p	37.8	2.3	miR-138-5p	39.9	0.2
miR-298-5p	38.0	3.5	miR-382-5p	39.9	0.2
miR-191a-5p	38.1	2.5	miR-212-3p	39.9	0.1
miR-148b-3p	38.2	0.8			

Supplemental Table III. Profile of upregulated and downregulated miRNAs in isCEC-exos compared with nCEC-exos.

Up-regulated miRNAs	Fold Change (>2)	P-value
miR-19a-3p	7.2	0.002
miR-27a-3p	5.7	0.006
miR-298-5p	5.1	0.009
miR-346	4.8	0.012
miR-125b-5p	4.7	0.013
miR-106b-5p	4.0	0.027
miR-195-5p	3.5	0.044
miR-34a-5p	3.4	0.014
miR-339-5p	3.1	0.021
miR-23a-3p	3.1	0.023
miR-93-5p	3.0	0.024
miR-126a-5p	2.8	0.034
miR-409a-3p	2.7	0.042
miR-15b-5p	2.4	0.009
miR-92a-3p	2.3	0.010
miR-20b-5p	2.3	0.011
let-7d-5p	2.3	0.012
miR-19b-3p	2.2	0.013
miR-146a-5p	2.2	0.014
miR-29a-3p	2.2	0.015
miR-488-3p	2.2	0.015
miR-139-5p	2.1	0.021
miR-26b-5p	2.0	0.023
miR-361-5p	2.0	0.025
Down-regulated miRNA	**Fold Change (<-2)**	**P-value**
miR-191a-5p	-2.0	0.030

Supplemental Table IV. Profile of upregulated miRNAs in axons treated with nCEC- exos compared with PBS.

Up-regulated miRNAs	Fold Change (>2)	P-value	Up-regulated miRNAs	Fold Change (>2)	P-value
miR-29c-3p	36.4	0.000	miR-150-5p	2.6	0.005
miR-298-5p	5.4	0.037	miR-484	2.5	0.006
miR-92a-3p	4.9	0.028	miR-126a-5p	2.5	0.007
miR-433-3p	4.8	0.029	miR-499-5p	2.5	0.007
miR-101b-3p	4.6	0.015	miR-148b-3p	2.4	0.008
miR-431	4.1	0.023	miR-511-5p	2.4	0.009
miR-381-3p	4.1	0.023	miR-106b-5p	2.3	0.010
miR-27a-3p	3.9	0.028	let-7b-5p	2.3	0.011
miR-203a-3p	3.7	0.035	miR-140-5p	2.3	0.011
miR-194-5p	3.5	0.043	miR-98-5p	2.3	0.011
miR-105	3.3	0.017	miR-489-3p	2.3	0.012
miR-342-3p	3.3	0.017	miR-338-3p	2.2	0.013
miR-337-3p	3.3	0.017	miR-39-3p	2.2	0.014
miR-33-5p	3.2	0.020	miR-29a-3p	2.2	0.016
miR-133b-3p	3.2	0.020	miR-146a-5p	2.2	0.016
miR-146b-5p	3.1	0.022	miR-134-5p	2.1	0.018
miR-598-3p	3.0	0.025	miR-339-5p	2.1	0.019
miR-20a-5p	2.7	0.042	miR-138-5p	2.1	0.020
miR-20b-5p	2.6	0.005	miR-107-3p	2.1	0.021
miR-29b-3p	2.6	0.005	let-7i-5p	2.0	0.022
miR-92b-3p	2.6	0.005			

Supplemental Table V. Profile of upregulated miRNAs in axons treated with isCEC-exos compared with PBS.

Up-regulated miRNAs	Fold Change (>2)	P-value	Up-regulated miRNAs	Fold Change (>2)	P-value
miR-29c-3p	159.9	0.000	miR-107-3p	8.7	0.019
miR-22-3p	84.8	0.000	miR-20b-5p	8.6	0.020
miR-29a-3p	47.4	0.000	miR-652-3p	8.3	0.023
miR-24-3p	46.2	0.000	miR-346	8.1	0.025
miR-181c-5p	45.6	0.000	miR-181d-5p	7.3	0.035
miR-93-5p	42.4	0.000	miR-30d-5p	7.2	0.038
let-7i-5p	32.1	0.001	miR-485-5p	7.1	0.039
miR-128-3p	29.8	0.001	miR-140-5p	7.0	0.015
miR-106b-5p	29.3	0.002	miR-511-5p	6.9	0.015
miR-181a-5p	27.8	0.001	miR-152-3p	6.3	0.022
miR-138-5p	25.7	0.001	miR-194-5p	6.1	0.024
miR-27a-3p	25.4	0.002	miR-15b-5p	5.9	0.027
miR-20a-5p	25.1	0.002	miR-9a-5p	5.9	0.028
miR-338-3p	24.2	0.002	miR-146a-5p	5.3	0.021
miR-125b-5p	23.8	0.002	miR-148b-3p	5.1	0.025
miR-19a-3p	20.8	0.003	miR-134-5p	4.9	0.027
miR-143-3p	19.5	0.013	miR-488-3p	4.9	0.028
miR-19b-3p	19.2	0.005	miR-105	4.3	0.045
miR-34a-5p	17.5	0.006	miR-126a-5p	4.2	0.005
miR-139-5p	17.5	0.007	miR-33-5p	4.1	0.006
miR-30e-5p	15.8	0.010	miR-98-5p	4.0	0.006
miR-212-3p	15.2	0.011	miR-337-3p	3.8	0.009
miR-124-3p	13.9	0.015	miR-431	3.7	0.010
miR-23a-3p	13.0	0.020	miR-342-3p	3.6	0.010
miR-195-5p	12.7	0.021	miR-433-3p	3.3	0.016
miR-101b-3p	12.7	0.021	miR-361-5p	3.3	0.017
miR-29b-3p	12.5	0.005	let-7b-5p	3.2	0.018
miR-132-3p	12.3	0.024	miR-39-3p	3.1	0.021
miR-130a-3p	11.8	0.027	miR-39-3p	3.0	0.007
miR-598-3p	11.7	0.028	miR-92b-3p	3.0	0.008
miR-484	11.4	0.031	miR-7a-5p	2.8	0.012
miR-376b-3p	11.0	0.002	miR-455-5p	2.7	0.013
miR-409a-3p	10.8	0.002	miR-382-5p	2.6	0.017
miR-30a-5p	10.3	0.003	miR-539-5p	2.5	0.019
miR-339-5p	10.2	0.003	miR-191a-5p	2.5	0.021
miR-298-5p	10.1	0.003	let-7d-5p	2.2	0.041
miR-150-5p	9.6	0.013	miR-133b-3p	2.2	0.027
miR-151-3p	8.9	0.017	miR-203a-3p	2.1	0.033

Supplemental Table VI. Profiles of up- and down-regulated miRNA in axons treated with isCEC-exos compared with nCEC-exos.

Up-regulated miRNAs	Fold Change (>2)	P-value	Up-regulated miRNAs	Fold Change (>2)	P-value
miR-29c-3p	30.3	0.000	miR-130a-3p	4.8	0.030
miR-22-3p	22.3	0.001	miR-143-3p	4.7	0.003
miR-125b-5p	18.3	0.003	miR-19a-3p	4.5	0.004
miR-181c-5p	16.8	0.004	miR-29b-3p	4.4	0.004
miR-181a-5p	16.8	0.004	miR-212-3p	4.0	0.006
miR-24-3p	16.0	0.004	miR-181d-5p	4.0	0.007
miR-128-3p	14.6	0.013	miR-101b-3p	3.8	0.008
miR-29a-3p	13.7	0.016	miR-598-3p	3.8	0.009
miR-93-5p	13.7	0.016	miR-652-3p	3.8	0.009
miR-30e-5p	12.4	0.023	miR-339-5p	3.5	0.003
let-7i-5p	12.1	0.025	miR-376b-3p	3.3	0.005
miR-338-3p	10.2	0.010	miR-151-3p	3.3	0.005
miR-195-5p	9.8	0.012	miR-150-5p	3.3	0.005
miR-23a-3p	9.6	0.013	miR-409a-3p	3.2	0.005
miR-106b-5p	9.0	0.017	miR-7a-5p	3.2	0.006
miR-138-5p	9.0	0.017	miR-191a-5p	3.2	0.006
miR-30a-5p	8.6	0.020	miR-15b-5p	3.0	0.008
miR-9a-5p	8.5	0.021	miR-346	2.9	0.009
miR-124-3p	7.9	0.027	miR-485-5p	2.9	0.009
miR-20a-5p	7.6	0.031	miR-107-3p	2.8	0.010
miR-34a-5p	6.9	0.028	miR-20b-5p	2.8	0.011
miR-132-3p	6.8	0.029	miR-152-3p	2.4	0.026
miR-27a-3p	6.7	0.030	miR-140-5p	2.2	0.016
miR-139-5p	6.1	0.042	miR-511-5p	2.1	0.020
miR-30d-5p	5.2	0.022	let-7d-5p	2.0	0.023
miR-19b-3p	5.0	0.027	miR-298-5p	2.0	0.011
miR-484	4.9	0.028			
Down-regulated miRNAs	**Fold Change (>2)**	**P-value**	**Down-regulated miRNAs**	**Fold Change (>2)**	**P-value**
miR-92a-3p	6.0	0.041	miR-489-3p	2.0	0.035
let-7e-5p	2.1	0.019	miR-499-5p	2.0	0.009

Supplemental Table VII. The precursor miRNA levels in CEC-exos.

	Ct values	
	nCEC-exos	isCEC-exos
pre-miR-19a	47.4 ±0.5	48.8±0.5
pre-miR-27a	48.5 ±0.3	48.3±0.3
pre-miR-298	47.4±2.3	48.8±1.0
pre-miR-195	50.4±0.3	52.5±2.6

*** Preclinical Checklist**

Preclinical Checklist: Prevention of bias is important for experimental cardiovascular research. ***This short checklist must be completed, and the answers should be clearly presented in the manuscript.*** *The checklist will be used by reviewers and editors and it will be published. See "Reporting Standard for Preclinical Studies of Stroke Therapy" and "Good Laboratory Practice: Preventing Introduction of Bias at the Bench" for more information.*

This study invovles animal models:
Yes

Experimental groups and study timeline

The experimental group(s) have been clearly defined in the article, including number of animals in each experimental arm of the study:	Yes
An account of the control group is provided, and number of animals in the control group has been reported. If no controls were used, the rationale has been stated:	Yes
An overall study timeline is provided:	Yes

Inclusion and exclusion criteria

A priori inclusion and exclusion criteria for tested animals were defined and have been reported in the article:	N/A

Randomization

Animals were randomly assigned to the experimental groups. If the work being submitted does not contain multiple experimental groups, or if random assignment was not used, adequate explanations have been provided:	N/A
Type and methods of randomization have been described:	N/A
Methods used for allocation concealment have been reported:	N/A

Blinding

Blinding procedures have been described with regard to masking of group/treatment assignment from the experimenter. The rationale for nonblinding of the experimenter has been provided, if such was not feasible:	N/A
Blinding procedures have been described with regard to masking of group assignment during outcome assessment:	N/A

Sample size and power calculations

Formal sample size and power calculations were conducted based on a priori determined outcome(s) and treatment effect, and the data have been reported. A formal size assessment was not conducted and a rationale has been provided:	N/A

Data reporting and statistical methods

Number of animals in each group: randomized, tested, lost to follow-up, or died have been reported. If the experimentation involves repeated measurements, the number of animals assessed at each time point is provided, for all experimental groups:	N/A
Baseline data on assessed outcome(s) for all experimental groups have been reported:	N/A
Details on important adverse events and death of animals during the course of experimentation have been provided, for all experimental arms:	N/A
Statistical methods used have been reported:	Yes
Numeric data on outcomes have been provided in text, or in a tabular format with the main article or as supplementary tables, in addition to the figures:	N/A

Experimental details, ethics, and funding statements

Details on experimentation including stroke model, formulation and dosage of therapeutic agent, site and route of administration, use of anesthesia and analgesia, temperature control during experimentation, and postprocedural monitoring have been described:	Yes
Different sex animals have been used. If not, the reason/justification is provided:	Yes

Statements on approval by ethics boards and ethical conduct of studies have been provided:	Yes
Statements on funding and conflicts of interests have been provided:	Yes

---

Date completed: 09/26/2020 07:05:33
User pid: 352370